Pressure of the metastable hard-sphere fluid

1997 J. Phys.: Condens. Matter 9 8591

(http://iopscience.iop.org/0953-8984/9/41/006)

J. Phys.: Condens. Matter **9** (1997) 8591–8599. Printed in the UK PII: S0953-8984(97)84923-5

Pressure of the metastable hard-sphere fluid

Robin J Speedy

Chemistry Department, Victoria University of Wellington, PO Box 600, Wellington, New Zealand

Received 4 June 1997, in final form 28 July 1997

Abstract. The pressure of the hard-sphere fluid was measured from near the equilibrium freezing density to the maximum density where the properties of the metastable fluid can be measured without it freezing or becoming glassy. Above the freezing density the measured pressures increase faster than the predictions of Padé approximants based on the known virial coefficients, which raises the possibility of a high-order singularity at the freezing density. However, a model fluid that has exactly the same virial coefficients as hard spheres, up to B_{16}, is shown to have a higher pressure than the hard-sphere fluid well below the freezing density of either fluid and this casts doubt on the reliability of Padé approximants.

1. Introduction

From an experimental point of view there is no sign that metastable phases are not continuous extensions of stable phases, yet careful theoretical analyses [1–4] predict a, very weak, essential singularity at the point where a stable phase becomes metastable. A simplistic explanation of the singularity is that 'droplets' of the less stable phase can form and decay freely within a stable phase but 'droplets' of the more stable phase must be excluded from the metastable phase, because they would grow and destroy it. The partition function for the stable phase therefore counts states that contain the 'droplets' but some constraint must be applied to exclude them from the partition function of the metastable phase. For a recent review of this topic and references the reader is referred to Debenedetti's book [5].

More virial coefficients are known [6–9] for hard spheres than for other fluids. The density range over which the virial expansion is valid has not been established but the general arguments suggesting an essential singularity at the freezing density of a fluid [1–5] imply that the virial expansion is not valid above the equilibrium freezing density.

The thermodynamic properties of the hard-sphere fluid [10–12] crystals [13–17] and glasses [10, 12, 18–20] have been studied extensively by computer simulation. The equation of state near the freezing density is shown in figure 1. To examine the possibility that the virial expansion may not extrapolate correctly through the equilibrium freezing density, the pressure of the metastable fluid was measured precisely and compared with pressures predicted by Padé approximants based on the known virial coefficients.

2. Methods and results

Fluids of $N = 500$ to $N = 4000$ spheres, of diameter σ, were simulated in a cubic cell of volume V with periodic boundaries using Alder and Wainwright's [10] algorithm and some efficiencies described by Lubachevsky and Stillinger [21]. The starting configuration,

0953-8984/97/418591+09$19.50

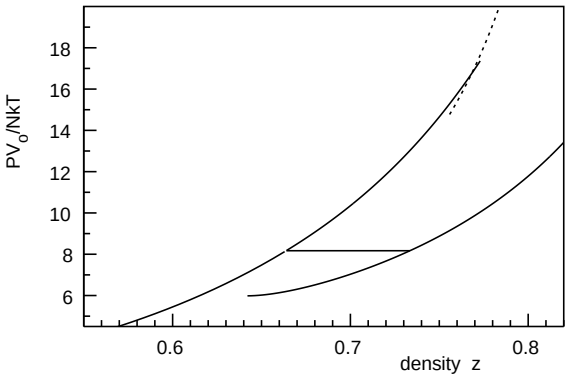

Figure 1. The pressure, $PV_0/NkT = zPV/NkT$, of hard spheres versus density $z = (N/V)\sigma^3/\sqrt{2}$ near the transition region [13–15]. For the face-centred cubic crystal $PV/NkT = 3/(1-z) - 0.5921(z-0.7072)/(z-0.601)$ [17] above the melting density and this equation extrapolates to a spinodal instability at $z = 0.64$. Equation (4) of this paper is used for the fluid. The dotted line shows the extrapolated pressure of annealed and reproducible glasses [18–20] $PV/NkT = 2.67/(1-z/0.8754)$. The fluid–crystal tie line is at $PV_0/NkT = 8.17\pm0.08$, where the density of the fluid is $z_f = 0.663\pm0.002$ and the density of the crystal is $z_c = 0.733\pm0.002$.

a face centred cubic crystal, was melted at low density to obtain an equilibrated fluid. The fluid was compressed with the method of Lubachevsky and Stillinger, in which the sphere diameter increases linearly with time during an otherwise normal molecular dynamics run. After compressing to density $z = (N/V)\sigma^3/\sqrt{2}$ the fluid was usually equilibrated for one million collisions (table 1) before starting a run in which the pressure was measured. The pressures listed in table 1 are about an order of magnitude more precise than Woodcock's values [12] up to $z = 0.73$, where it was possible to simulate the fluid for 10^8 collisions without freezing. They agree with Woodcock's values [12] up to $z = 0.74$. At higher densities Woodcock's pressures are lower, suggesting that his fluid and glass were partly frozen. For $z > 0.73$, less precise results, averaged over several short runs, are reported to $z = 0.77$. The properties of hard-sphere glasses are reported elsewhere [18, 19].

3. Freezing

Fluids of $N = 1372$ spheres were simulated for 10^8 collisions without freezing, up to the density $z = 0.73$. At higher density they always froze within a few million collisions and the pressure was averaged over several short runs, as shown in figure 2. For the short runs the fluid was simulated for half a million collisions at $z = 0.5$ and then compressed to $z = 0.74$, 0.75, 0.76 or 0.77, where the pressure was followed with time for 2 to 5 million collisions. The estimated equilibrium pressure of the fluid, shown by the horizontal lines in figure 2, is an average over the last 1 to 2 million collisions of three or more runs in which the pressure remained stable and in which the average pressures agreed to within 0.1 in PV/NkT. At $z = 0.74$ the root-mean-square displacement of the spheres is near one diameter in a run of 2 million collisions, but when $z = 0.76$ it is only 0.5σ and the system is glassy on the simulation time scale.

The downward pressure drift immediately after the compression, shown in figure 2, is due to relaxation of the fluid, or glass, and the pressure drops at longer times are due to

Table 1. The pressure PV/NkT of the hard-sphere fluid. N is the number of spheres, N_{eq} is the equilibration period (after compressing an equilibrated configuration from a lower density) in millions of collisions, N_c is the run length in millions of collisions. The density relative to that of the close packed crystal is $z = (N/V)\sigma^3/\sqrt{2}$. When $z \leqslant 0.735$ the estimated error in the last two digits of PV/NkT, shown in brackets, is $2\sqrt{\delta^2}/\sqrt{N_s}$ where δ^2 is the rms variation in values of PV/NkT calculated in $N_s = 20$ sub-intervals of the run. At higher densities the error estimates are based on the agreement between several independent runs.

N	N_{eq}	N_c	z	PV/NkT
1372	5	40	0.625	10.203(03)
1372	2	100	0.650	11.498(04)
1372	1	100	0.680	13.341(04)
1372	1	100	0.690	14.039(05)
1372	5	100	0.700	14.787(04)
4000	1	20	0.700	14.786(11)
1372	1	100	0.705	15.187(08)
1372	1	50	0.710	15.587(10)
1372	10	100	0.715	16.020(10)
1372	1	100	0.720	16.457(08)
4000	1	20	0.720	16.458(26)
1372	1	100	0.725	16.904(11)
1372	1	100	0.730	17.351(19)
4000	1	50	0.730	17.370(21)
1372	1	10	0.735	17.905(40)
1372	0.5	14×1	0.740	18.42(05)
1372	0.5	3×2	0.750	19.55(10)
1372	1	3×2	0.760	21.05(10)
1372	1	3×2	0.770	22.40(15)

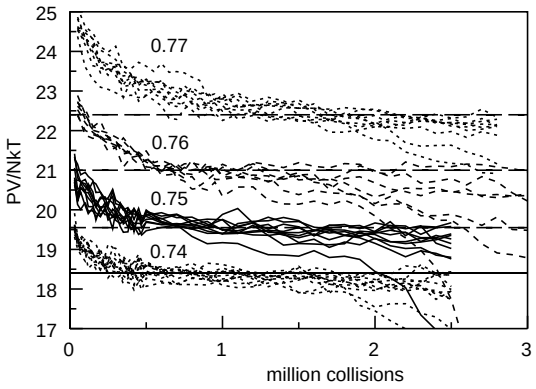

Figure 2. Variation of PV/NkT with time, measured in millions of collisions, for the hard-sphere fluid. Each run was started by compressing a different fluid configuration from $z = 0.5$ to the density shown. Pressures shown are averaged over intervals of 10^5 collisions. Many more runs of different length are not shown. The initial downward drift is due to relaxation after the compression and at longer times it is due to freezing. Horizontal lines show estimated fluid pressures, averaged over selected runs in which the pressure did not drift during the last 2 million collisions and which agreed with each other to within ± 0.1 in PV/NkT.

freezing. The time scales for these two processes are about the same at the densities shown in figure 2 so the properties of the metastable state may not be not well defined [3].

Smaller systems freeze quicker than larger ones, which means that the periodic boundaries in a small system encourage crystallization. If freezing depends on random and local nucleation events then the probability $P_f(N,t)$ that a supercooled fluid of N spheres will freeze in a time t, should increase in proportion to the simulation time and to the system size, so that $P_f(N,t)$ is proportional to Nt. Figure 3 shows the density where fluids of N spheres freeze in runs of $N_c = 250\,000$ and 10 million collisions. The collision rate per sphere is independent of system size, so the simulation time t scales as N_c/N, and Nt is constant when N_c is fixed. Thus, the lines in figure 3 would be horizontal if $P_f(N,t)$ varied as Nt. The negative slopes show that the probability of freezing in a given time decreases as the system size increases, which is consistent with the conclusions of more detailed studies [22, 23] of freezing in Lennard–Jones fluids.

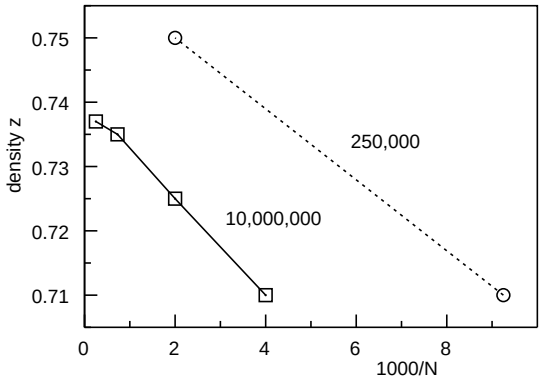

Figure 3. The lowest density where the hard-sphere fluid usually freezes in runs of 0.25 million and 10 million collisions, plotted against $1000/N$ where N is the number of spheres. The lines would be horizontal if freezing occurred by random nucleation. The negative slopes show that small systems freeze at lower densities than larger ones, indicating that the periodic boundaries influence crystallization.

Pressures reported by Rintoul and Torquato [24] near $z = 0.756$ and 0.77 are 1.9% higher than the present values. They evidently fitted pressures measured during the initial short-time relaxation to an exponential decay with time to estimate the equilibrium value. They state that, at higher densities, larger systems freeze faster than smaller ones, which is the opposite of the trend shown in figure 3.

4. Equation of state

The known viral coefficients [6–9], B_k, in the virial expansion [25, 26]

$$PV/NkT = 1 + \sum_{k=2} B_k \rho^{k-1} \tag{1}$$

where $\rho = N/V$, are listed in table 2.

Many analytic equations of state have been proposed for the hard-sphere fluid [27]. The precise pressure measurements at low density by Erpenbeck and Wood's [11] eliminate many of the older equations from further consideration and Janse van Rensburg's [9] calculation of B_8 eliminates most others.

Table 2. Values of the virial coefficients B_k from Janse van Rensburg [9] and the constants a_k and c_k in the $P(3, 2)$ equation of state, equation (2). $B_2 = (2/3)\pi\sigma^3$. The value $B_6/B_2^5 = 0.038\,82$ was chosen to best fit the measured pressures, as described in the text. Deviations are shown in figures 4 and 5. The $P(3, 2)$ equation implies that $B_7/B_2^6 = 0.012\,97$ and $B_8/B_2^7 = 0.004\,185$.

k	B_k/B_2^{k-1}	a_k	c_k
1		1.0	−0.548 986
2	1	0.076 014	0.075 647
3	5/8	0.019 480	
4	0.286 9495		
5	0.110 252(1)		
6	0.038 808(55)		
7	0.013 071(70)		
8	0.004 32(10)		

The pressure calculated from equation (1), truncated after B_8, is a few per cent too low near the freezing density. A popular [9, 11, 14] method of estimating and summing the higher terms is to express the equation of state as a Padé approximant

$$PV/NkT = P(m, n) = 1 + (x + a_2x^2 + \cdots + a_mx^m)/(1 + c_1x + \cdots + c_nx^n) \tag{2}$$

in which $x = B_2\rho$ and up to seven of the constants a_k and c_k are determined by the known virial coefficients B_2 to B_8 listed in table 2. The $P(m, n)$ reported by Janse van Rensburg [9] use the virial coefficients without any allowance for their uncertainties. The resulting equations of state (equations (3.5) to (3.8) of [9]) are not in good agreement with each other and they do not predict the measured pressures accurately at densities $z > 0.5$. To optimize the Padé equations of state, B_6, B_7 and B_8 were each varied, over the range $\pm 1.5E_k$, where E_k is the numerical uncertainty in B_k, and the Padé coefficients were obtained from the simultaneous equations that relate them to the B_k. The resulting equations of state were then compared with the simulation data. In order to weight the measured pressures according to their precision, the deviation, $\delta = (PV/NkT - P(m, n))/E_P$, where E_P is the uncertainty in PV/NkT, was calculated at each density. Minimizing the sum $\Sigma\delta^2$, for densities $z \leqslant 0.68$, determines the best-fit parameters in $P(m, n)$. The parameters for $P(3, 2)$ are listed in table 2. Figure 4 shows that $P(3, 2)$ reproduces the low-density data of Erpenbeck and Wood to within twice the very small experimental errors that they report, and it fits the present results, to within the errors listed in table 1, up to $z = 0.68$, which is just above the equilibrium freezing density, $z_f = 0.663$. Quantitatively very similar results were obtained with $P(4, 2)$, $P(3, 3)$ and $P(5, 2)$ but the quality of the fit is not significantly improved over that of $P(3, 2)$. These $P(m, n)$ are all consistent with the known B_k to within $\pm 1.5E_k$, and they all predict that $B_9/B_2^8 = 0.001\,32 \pm 0.000\,01$ and $B_{10}/B_2^9 = 0.000\,407 \pm 0.000\,004$. Furthermore, extrapolation of all the fitted $P(m, n)$ to densities up to $z = 0.76$ yields the same pressure, to within ± 0.03 in PV/NkT (whereas equations (3.5) to (3.8) of [9] differ by 1 in PV/NkT at $z = 0.76$).

A common feature of the fitted equations is that they reproduce the known virial coefficients, and the measured pressures up to the freezing density, but extrapolation to higher density yields pressures that are lower than the measured values, as shown in figure 4. Attempts to choose the Padé parameters to fit the higher-density data resulted in significant systematic deviations from the measured pressures and inconsistencies with the virial coefficients.

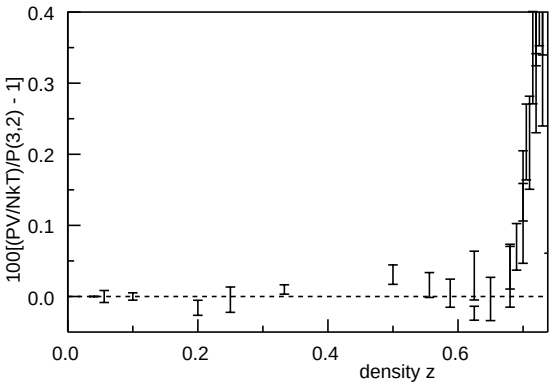

Figure 4. Percentage deviation of measured values of PV/NkT from the $P(3, 2)$ approximant (equation (2)) versus density. Pressures at densities $z \leqslant 0.625$ are from Erpenbeck and Wood [11] and at $z \geqslant 0.625$ they are from table 1. The coefficients of $P(3, 2)$ are listed in table 2. Above the freezing density, $z_f = 0.663$, the deviations are systematic (figure 5).

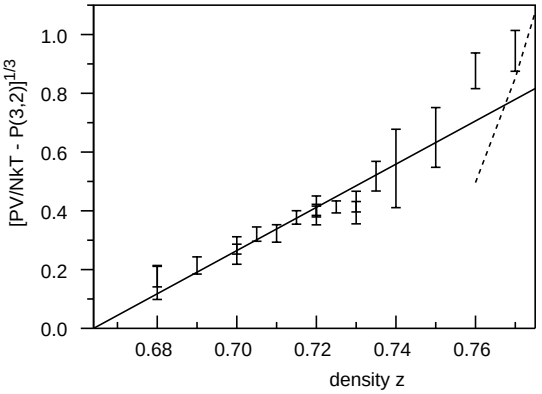

Figure 5. Cube root of the deviation of the measured values of PV/NkT (table 1) from the Padé approximant $P(3, 2)$ at densities z above the freezing density $z_f = 0.663$. Deviations from $P(4, 2)$, $P(3, 3)$, $P(4, 3)$ and $P(5, 2)$ are the same to within the errors shown. The solid line corresponds to equation (3). The dotted line shows the extrapolated pressure of the reproducible glasses [18–20].

Figure 5 shows that, above the freezing density, $[PV/NkT - P(3, 2)]^{1/3}$ varies linearly with density and extrapolates to zero at the freezing density, which means that the deviations vary as the cube of the distance above the freezing density. The deviations are described by

$$D(z) = PV/NkT - P(3, 2) = 400(z - z_f)^3 \tag{3}$$

where $z_f = 0.663$ is the equilibrium freezing density. Figures 4 and 5 show that the equation of state of the hard-sphere fluid can be expressed as

$$PV/NkT = \begin{cases} P(3, 2) & 0 < z < z_f \\ P(3, 2) + D(z) & z_f < z \leqslant 0.75. \end{cases} \tag{4}$$

According to equations (3) and (4), the third derivatives of the pressure, or the fourth derivatives of the free energy, change discontinuously when the stable fluid becomes metastable.

A possible interpretation of equation (4) is that the Padé approximants based on the known B_k do not sum the tail of the series accurately, so that when more virial coefficients are known the Padé approximants will change and they may then account for the high-density data. Evidence against this possibility is that the different $P(m, n)$ extrapolate to $z = 0.76$ in the same way, and that they predict the same B_9 and B_{10}.

A second interpretation of equation (4) is that the Padé approximants sum the tail of the viral series accurately, but that the virial expansion is not valid above the freezing density. This is consistent with the notion that there is an essential singularity at the freezing density.

Section 5 reports an attempt to distinguish between those two possibilities, by simulating some constrained model fluids, one of which has exactly the same virial coefficients as the hard-sphere fluid up to B_{16}.

Equation (4) can be integrated analytically to get the entropy, relative to an ideal gas, from

$$\Delta_{ig}S/Nk = -\int_0^z (PV/NkT - 1)d\ln\{z\} \tag{5}$$

so it is not necessary to develop a separate Padé approximant for the entropy [9, 14] and all the thermodynamic properties of the fluid can be obtained from equations (2) to (5) with the parameters in table 2. As a check, the equilibrium melting pressure of the face-centred cubic crystal [17] was recalculated. The results, given in the legend to figure 1, are little lower than the values of Hoover and Ree [14] but they agree to within the combined uncertainties.

Ross and Alder [28] noted that the equilibrium freezing density of fluids coincides with the lowest density where the crystal survives without melting in simulation studies. Hard-sphere crystals can be simulated for a few million collisions at $z = 0.67$ before melting but they melt quickly at $z = 0.66$. It is interesting that the highest density where the fluid can be simulated without freezing, $z = 0.73$, is also close to the equilibrium melting density of the crystal. These 'rules' probably stem from the difficulty of fitting coexisting phases in a small cell with periodic boundaries.

5. Constrained simulations

Constraints are commonly used in simulations to stabilize metastable states and facilitate entropy measurements [14, 15, 20]. Cell model constraints can prevent hard-sphere crystals from melting [14] and constraining the size of voids can prevent superheated Lennard–Jones fluids from boiling [5, 29, 30]. The favoured method of avoiding freezing in simulations has been to use mixtures [31], rather than a constraint, and little is known about the kind of constraints that might prevent freezing or the effect that they have on the properties of the constrained fluid. This section investigates the effect of a very simple constraint, designed to inhibit freezing of the hard-sphere fluid.

In the crystal, each sphere has 12 close neighbours so a constraint that prevents a sphere from having 12 close neighbours in the fluid may inhibit freezing. The neighbours of a sphere are defined as those whose centres are within a distance $\lambda\sigma$, where λ can be varied to optimize the constraint. Similarly, constraints that limit the number of second or third neighbours of a sphere may inhibit freezing. These constrained systems are easy to simulate using a saturated square well model [32] SSW($N_v, \lambda, \epsilon/kT = 0$) with valency N_v, well diameter $\lambda\sigma$ and well depth $\epsilon = 0$. The simulations proceed as for hard spheres except that lists are kept of the neighbours of each sphere and, when a sphere already has N_v neighbours, other spheres bounce off it, as though they are both hard spheres of diameter

of $\lambda\sigma$. The constraint has no effect if N_v is larger than the number of spheres that can be packed within $\lambda\sigma$ of a sphere.

One reason for choosing this kind of constraint is that it has no effect on clusters of up to $N_v + 1$ spheres. The virial coefficients B_k can be expressed in terms of the configuration integrals for $j = 1, 2, \ldots, k$ spheres, without assuming pairwise additivity [26], which means that the B_k, for $k \leqslant N_v + 1$, are exactly the same for the SSW($N_v, \lambda, \epsilon/kT = 0$) fluid and for the hard-sphere fluid. If the two fluids have different pressures then it follows that any method of summing the virial series, based on the exact B_k, $k \leqslant N_v + 1$, does not sum the virial series accurately above the density where the pressures differ, or that the virial expansion is not valid above that density.

The excess pressure of some SSW models, relative to the hard-sphere fluid, represented by $P(3, 2)$, is shown in figure 6. In general the severity of the constraint increases, and the pressure increases, if λ is increased or N_v is decreased. The models shown in figure 6 all showed signs of freezing to defective crystals when simulated near $z = 0.74$ for several million collisions, so the constraints studied are not effective in preventing freezing.

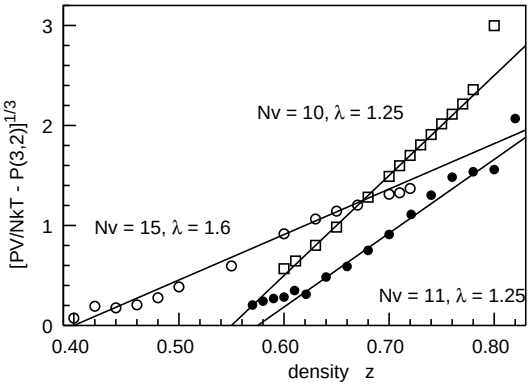

Figure 6. Cube root of the deviation of the measured values of PV/NkT, for some SSW($N_v, \lambda, \epsilon/kT = 0$) fluids, from the Padé approximant $P(3, 2)$ at density z. $P(3, 2)$ represents PV/NkT for hard spheres when $z < 0.68$. The lines correspond to $PV/NkT = P(3, 2) + C(z - z_1)^3$ with $C = 400$ and $z_1 = 0.575$ for $N_v = 11$, $\lambda = 1.25$, $C = 1000$ and $z_1 = 0.55$ for $N_v = 10$, $\lambda = 1.25$; $C = 108$ and $z_1 = 0.40$ for $N_v = 15$, $\lambda = 1.6$.

The constrained models have significantly higher pressures than the hard-sphere fluid well below the freezing density of either fluid. For instance, the pressure of the SSW($N_v = 15, \lambda = 1.6, \epsilon/kT = 0$) fluid is higher than that of hard spheres when $z > 0.45$ and it is most unlikely that any crystalline phase is more stable than the fluid at such low density, where $PV/NkT < 5$. This shows that even if 16 virial coefficients are known exactly, a Padé, or any other approximant based on the 16 virial coefficients, cannot be relied on to predict the equation of state accurately up to the freezing density.

6. Conclusion

The evidence for a singularity at the hard-sphere fluid freezing density, suggested by figures 4 and 5, is inconclusive because it relies on the assumption that the Padé approximants accurately represent the tail of the virial series. When hard spheres are considered in isolation, as in section 4, that assumption seems plausible and it is supported by the good agreement between several different $P(m, n)$ that agree with the known virial

coefficients and with the pressure measurements, up to the freezing density. However, a saturated square well fluid that has the same virial coefficients as the hard-sphere fluid, up to B_{16}, has a higher pressure than the hard-sphere fluid when $z > 0.45$. This shows that either the virial expansion is not applicable when $z > 0.45$ or that knowledge of the coefficients beyond B_{16} is required to predict the pressure reliably. In either case, Padé approximants based on the virial coefficients up to B_{16} cannot be relied on to predict the pressure accurately.

Acknowledgment

This work was supported by the Marsden Fund through contract GRN 501.

References

[1] Fisher M E 1967 *Physics* **3** 255
[2] Fisher M E 1967 *Rep. Prog. Phys.* **30** 615
[3] Langer J S 1974 *Physica* **73** 61
[4] Binder K 1987 *Rep. Prog. Phys.* **50** 783
[5] Debenedetti P G 1996 *Metastable Liquids* (Princeton, NJ: Princeton University Press)
[6] Ree F H and Hoover W G 1964 *J. Chem. Phys.* **40** 939
[7] Ree F H and Hoover W G 1967 *J. Chem. Phys.* **46** 4181
[8] Kratky K W 1982 *J Stat. Phys.* **27** 533
Kratky K W 1982 *J. Stat. Phys.* **29** 129
[9] Janse van Rensburg E J 1993 *J. Phys. A: Math. Gen.* **26** 4805
[10] Alder B J and Wainwright T E 1960 *J. Chem. Phys.* **33** 1439
[11] Erpenbeck J J and Wood W W 1984 *J. Stat. Phys.* **35** 321
[12] Woodcock L V 1981 *Ann. NY Acad. Sci.* **371** 274
[13] Alder B J, Hoover W G and Young D A 1969 *Phys. Rev.* **183** 83
[14] Hoover W G and Ree F H 1968 *J. Chem. Phys.* **49** 3609
[15] Frenkel D and Ladd A J C 1984 *J. Chem. Phys.* **81** 3188
[16] Woodcock L V 1997 *Nature* **385** 141
[17] Speedy R J 1997 unpublished
[18] Speedy R J 1994 *J. Chem. Phys.* **100** 6684
[19] Speedy R J 1994 *Mol. Phys.* **83** 591
[20] Speedy R J 1993 *Mol. Phys.* **80** 1105
[21] Lubachevsy B D and Stillinger F H 1990 *J. Stat. Phys.* **60** 561
[22] Honeycutt J D and Andersen H C 1986 *J. Phys. Chem.* **90** 1585
[23] Swope W C and Andersen H C 1990 *Phys. Rev.* B **41** 7042
[24] Rintoul M D and Torquato S 1996 *Phys. Rev. Lett.* **77** 4198
[25] Mayer J E and Mayer M G 1940 *Statistical Mechanics* (New York: Wiley)
[26] Hill T L 1987 *Statistical Mechanics: Principles and Selected Applications* (New York: Dover)
[27] Boublík T and Nezbeda I 1985 *Coll. Czech. Chem. Commun.* **51** 2301
[28] Ross M and Alder B J 1966 *Phys. Rev. Lett.* **16** 1077
[29] Corti D S and Debenedetti P G 1995 *Ind. Eng. Chem. Res.* **34** 3573
[30] Corti D S, Debenedetti P G, Sastry S and Stillinger F H 1997 *Phys. Rev.* E **55** 5522
[31] Kobb W and Andersen H C 1994 *Phys. Rev. Lett.* **73** 1376
[32] Speedy R J 1992 *J. Phys. Chem.* **97** 2723